

The role of feedback in shaping neural representations in cat visual cortex

Ralf A. W. Galuske^{*†}, Kerstin E. Schmidt^{*}, Rainer Goebel[‡], Stephen G. Lomber[§], and Bertram R. Payne[¶]

^{*}Department of Neurophysiology, Max Planck Institute for Brain Research, 60528 Frankfurt am Main, Germany; [‡]Department of Psychology, University of Maastricht, 6229ER Maastricht, The Netherlands; [§]Cerebral Systems Laboratory, School of Behavioral and Brain Sciences, University of Texas at Dallas, Richardson, TX 75083-0688; and [¶]Laboratory of Visual Perception and Cognition, Center for Advanced Biomedical Research, Boston University School of Medicine, Boston, MA 02118–2526

Edited by Charles G. Gross, Princeton University, Princeton, NJ, and approved October 7, 2002 (received for review July 4, 2002)

In the primary visual cortex, neurons with similar response preferences are grouped into domains forming continuous maps of stimulus orientation and direction of movement. These properties are widely believed to result from the combination of ascending and lateral interactions in the visual system. We have tested this view by examining the influence of deactivating feedback signals descending from the visuoparietal cortex on the emergence of these response properties and representations in cat area 18. We thermally deactivated the dominant motion-processing region of the visuoparietal cortex and used optical and electrophysiological methods to assay neural activity evoked in area 18 by stimulation with moving gratings and fields of coherently moving randomly distributed dots. Feedback deactivation decreased signal strength in both orientation and direction maps and virtually abolished the global layout of direction maps, whereas the basic structure of the orientation maps was preserved. These findings could be accounted for by a selective silencing of highly direction-selective neurons and by the redirection of preferences of less selective neurons. Our data suggest that signals fed back from the visuoparietal cortex strongly contribute to the emergence of direction selectivity in early visual areas. Thus we propose that higher cortical areas have significant influence over fundamental neuronal properties as they emerge in lower areas.

In each cerebral cortical area, neurons have a unique inventory of receptive field properties, and each property is combined with that of its neighbors to form orderly representations of stimulus features; these different representations are overlain within the same population of neurons. Neurons in early visual areas are selective for the orientation and direction of movement of visual stimuli. Both features are represented at the level of individual neurons as well as of spatially organized representations as orientation and direction maps. These features are widely believed to emerge by the particular combinations of ascending and lateral interactions (1–4). However, there are equally prominent projections descending from higher visual areas onto the same region. Even though limited evidence suggests that individual neurons in early cortical structures are influenced by feedback signals from higher areas (5–7), the impact of deactivating cortical feedback pathways on direction and orientation selectivities and their representations spanning a large population of neurons has not been studied (8).

The middle suprasylvian (MS) cortex in the visuoparietal region is critical for the discrimination of movement direction and extraction of structure from motion (9, 10). Neurons within the region (Fig. 1*a*) are particularly sensitive to movement, movement direction, and line orientation (11–14), and send a prominent projection to area 18 (15–17). Therefore, these neurons could contribute significantly to the emergence of both direction of movement and orientation selectivity in this area. We tested this hypothesis by cooling MS cortex and, thus, silencing the origins of projections to area 18, and assaying the impact of the deactivation by electrophysiological recordings and optical imaging of intrinsic signals in area 18 (Fig. 1*b*).

Materials and Methods

Animal Preparation. Cooling loops (18) were implanted into the posterior MS (pMS) sulcus of five cats. Four of these animals also had a second loop placed over one of the following sites: primary auditory cortex, area 7, or posterior ectosylvian (PE) cortex (Fig. 1*a*). Imaging chambers were positioned over area 18 (centered in the midline at AP0) on the marginal gyrus. Cryoloops and chambers were implanted under anesthesia with nitrous oxide and halothane. The effectiveness of the pMS cooling loops was verified behaviorally in a visual field perimetry test (19), which tests for deactivation of the superficial and deeper layers (20). All cats neglected visual stimuli presented in the contralateral, but not ipsilateral, hemifield when the cryoloops were cooled to 1–3°C. Four to 10 weeks after loop implantation, the cats were reanesthetized and prepared for optical and electrophysiological recording. Anesthesia was initiated by intramuscular injection of ketamine (10 mg/kg) and xylazine (1 mg/kg) and maintained after tracheotomy by artificial ventilation with a mixture of N₂O (70%), O₂ (30%), and halothane (0.8%) and a systemic muscle relaxant (pancuronium, 0.8 mg/h) was administered to prevent eye movements. All animal experiments were performed in accordance with the guidelines for the use of animals in research of the Society for Neuroscience. In addition, two cats without cooling probes were optically recorded as described above to determine the properties of intrinsic signal imaging in the absence of visual stimulation.

Visual Stimulation. Visual stimuli were presented on a 21-in computer screen (refresh rate 100 Hz) at a distance of 57 cm. Maps of orientation and direction preference were obtained by optical imaging of intrinsic signals evoked by whole-field high-contrast gratings with a periodicity of 0.15 cycles per degree moving at four orientations (0, 45, 90, and 135°) at a velocity of 16°/s in the two directions orthogonal to the grating orientation. Direction preference maps were obtained by stimulation with gratings and fields of randomly positioned dots (2.83 dots/in²) moved coherently in eight different directions at 16°/s. Within each set of eight different stimuli, the presentation sequence was randomized.

Optical Data Acquisition. For optical imaging, chambers were filled with silicone oil and sealed with a glass plate. Intrinsic signals evoked by the stimuli were detected with a cooled charge-coupled device camera system (ora2001, Optical Imaging Europe, Munich) under illumination with light of a wavelength of 620 nm. The camera was fitted with a lens system consisting of two 50-mm Nikon objectives and a ×2 extender providing a 4 × 5-mm field of view. Stimuli were presented for 9 s, and camera

This paper was submitted directly (Track II) to the PNAS office.

Abbreviations: MS, middle suprasylvian; pMS, posterior MS; PE, posterior ectosylvian; MDI, mean direction index.

[†]To whom correspondence should be addressed. E-mail: galuske@mpi-hfrankfurt.mpg.de.

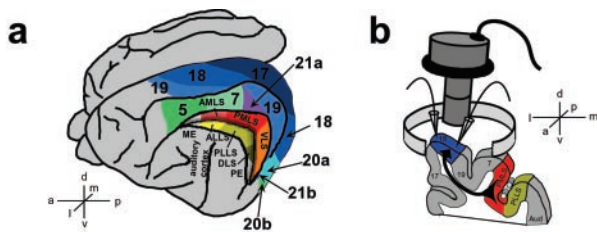


Fig. 1. (a) Schematic dorsolateral view of the cat brain to show positions of primary and higher order visual areas and those of nonvisual areas that were used for control coolings. ME indicates middle ectosylvian and PE indicates posterior ectosylvian cortex (adapted from ref. 51). (b) Schematic drawing of a coronal section to show deactivated pMS cortex and the assay site in area 18. The arrow represents feedback projections from pMS (posteromedial lateral suprasylvian, posterolateral lateral suprasylvian) cortex to area 18.

frames were collected during the entire stimulation period. Usually, data were averaged for ≈ 20 – 30 min for each phase of feedback manipulation, and sets of stimuli were presented 16 times.

Optical Data Analysis. Unless stated otherwise, orientation and direction maps were calculated by normalization to the sum of all different stimulation conditions (“cocktail blank”). In a limited number of experiments, we also acquired images from the cortex in the absence of specific visual stimulation (“blanks”). The number of blanks in each set of stimuli was always matched to the number of different stimulus conditions. In these cases, we normalized the single-condition maps to the average of the “blank” trials. Images were filtered with a high pass of 50 pixel and a low pass of 5 pixel. For the construction of orientation maps, the activity maps obtained with the like oriented but differently moving gratings were added. Clipping values for single-condition orientation and direction maps were fixed during one data set from baseline to recovery and were usually in the range of 0.001–0.002. From the single-condition maps, preferred angles of orientation and direction were calculated by pixelwise vectorial addition of the activity in the single-condition maps. For the gratings, we additionally assigned the strongest response of each pixel as the preferred direction. For quantification of response selectivity, we calculated the vector strength for each pixel. This value ranges between 0 and 1 and was calculated pixelwise by dividing the length of each resultant vector by the sum of all activities. For display, the orientation and direction preference are color coded and, in some cases, supplemented with data on response selectivity by incorporating pixel brightness to represent the respective vector strength (polar maps).

Electrophysiological Recordings. For the electrophysiological recordings, up to six tungsten microelectrodes were simultaneously inserted into area 18. Activity of individual neurons was isolated by thresholding and stored as time stamps. Visual stimulation periods were 2 s in duration. Stimulation was performed with the same set of oriented gratings moving in eight different directions as for the optical imaging. Recordings were initiated 500 ms before stimulus onset and continued for 500 ms after offset of stimulation. During each set of recordings, each stimulus condition was repeated 20 times. One baseline-cooling-recovery cycle consisted of three 20-min periods. Individual responses were calculated over the whole stimulation period and the spontaneous activity as measured in the period before onset of stimulation was subtracted. For the quantification, the same methods as in the optical imaging were used to describe orientation preference and selectivity. For direction, we additionally

calculated the mean direction index (MDI), as suggested by Orban *et al.* (21).

Results

Effects on Orientation Maps. Orientation maps in area 18 were obtained by stimulation with moving gratings. During periods of feedback deactivation, the general layout of these maps was maintained (Fig. 2*a* and *b*), and the topographic organization of map features, such as pinwheels and fractures, remained stable (Fig. 2*b*). However, response strength (Fig. 2*a* and *c*), and orientation selectivity were all reduced (Fig. 2*b* and *d*) but returned toward predeactivation levels within 30 min after onset of rewarming after the cessation of pMS cooling (Fig. 2*b*). The cooling-induced decreases in signal and vector strengths were consistent over all 25 cooling cycles performed in five different cats and averaged 16% and 52%, respectively (Fig. 2*e*). In contrast, direction maps calculated from stimulation with unidirectionally moving oriented gratings during feedback deactivation differed substantially from direction maps obtained with the same set of stimuli under conditions of intact feedback. In these maps, direction preference could change by values up to 180° , whereas the underlying orientation domains remained unchanged (Fig. 2*f* and *g*).

Effects on Direction Maps. To examine the impact of feedback removal on the representation of direction of motion in the absence of contour orientation, direction preference maps were generated by stimulation with fields of coherently moving dots. Feedback deactivation reduced both signal and vector strengths in the maps generated with these stimuli (Fig. 3*a*–*c*), as was the case for orientation, and in averages taken across 15 cooling sessions in 5 cats the reductions were in the range of 10 and 40%, respectively (Fig. 3*g*). As already seen with gratings (Fig. 2*f* and *g*), feedback deactivation also disrupted the principal layout of the direction maps (Fig. 3*b*, *d*, and *e*). Pixelwise comparison of the direction preference revealed striking alterations in the representation of movement direction during feedback removal (Fig. 3*d*–*f*) and altered properties even in the most direction-selective regions (Fig. 2*g*). There was little systematic relationship between the direction maps generated before and during feedback removal ($r = 0.209$, $P < 0.0001$). By silencing pMS cortex, regions of high direction selectivity and positions of fractures could be shifted (Fig. 3*b*). Within each set of maps taken under the same condition direction representations were stable, as indicated by the high correlation between maps calculated from individual frames at different times during stimulation (Fig. 3*e*). After rewarming the pMS cortex, direction maps generated by both gratings (Fig. 2*f* and *g*) and random dots (Fig. 3*b*, *d*, and *f*) regained features identified before pMS deactivation. The correlation values were in the range of 0.5–0.6, which is comparable to the range seen in other studies (e.g., ref. 22). These findings were consistent over all 15 cooling cycles performed during stimulation with random dots in five different cats (Fig. 3*f* and *g*). To further exclude the possibility that the observed changes in the direction maps were based only on changes in cortical activation and thus signal-to-noise ratio, we additionally compared the correlation values among stimulated frames with and without cooling to those obtained in the absence of visual stimulation in two cats (Fig. 3*e*). This comparison revealed that the correlation values between individual frames in both the presence or absence of feedback from pMS cortex were markedly higher than in recordings without visual stimulation.

Effects on Individual Neurons. Extracellular single-neuron recordings in two of the same cats confirmed the impact of silencing the pMS cortex on area 18 (Fig. 4). In recordings taken from the upper cortical layers, we identified highly direction-selective neurons that were virtually silenced by cooling of the pMS cortex

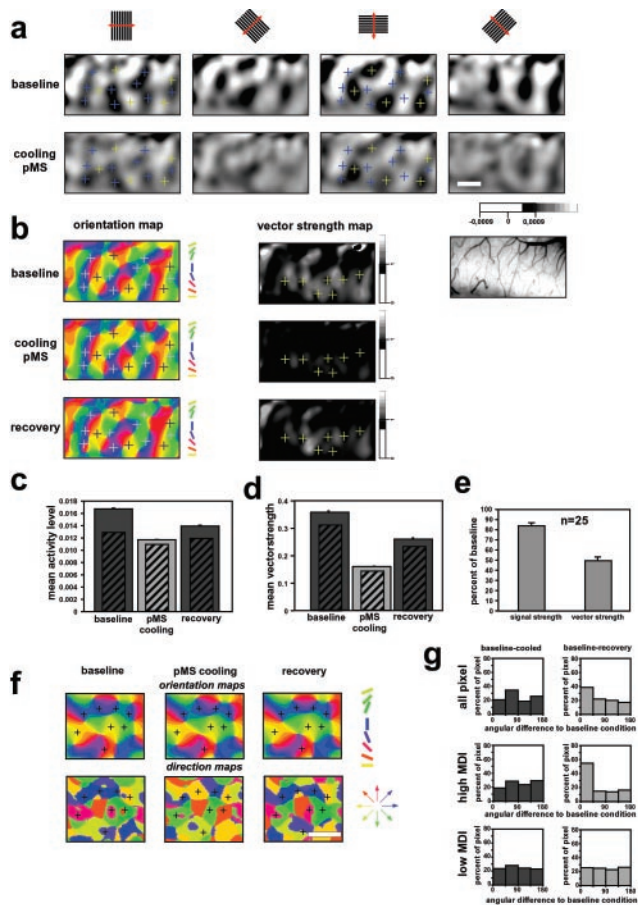


Fig. 2. (a–e) Impact of feedback removal on orientation maps. (a) Single-condition orientation preference maps recorded in area 18 before (Upper) and during (Lower) cooling deactivation of pMS cortex. The orientations are indicated on top of each column of images. (Bar = 1 mm.) The gray scale below indicates the coding of the signal ranges. Single-condition maps were normalized to the “blank” condition. The crosses identify regions that were well activated by either vertically (blue) or horizontally (yellow) oriented stimuli. (b) Orientation preference (Left) and vector strength (Right) map pairs before, during, and after cooling deactivation of pMS cortex from the experiment shown in a. Preferred angles are color-coded according to the scheme below the left column. The blue and yellow crosses in a are exchanged by light- and dark-gray crosses, respectively, in the orientation maps. The vector strength maps are coded according to the scale bar shown below the right column. Crosses in the vector strength map mark the persistent regions of low vector strength around pinwheels during the cooling of pMS cortex. The rightmost panel is a video capture of the imaged region. (c) Averages of absolute response level of the example shown in a. Filled bars indicate results from “blank” normalization. Hatched inset bars indicate results from “cocktail blank” normalization of the same data set. (d) Averages of vector strength levels. (e) Average changes in percent of baseline of response strength and vector strength averaged over the whole set of experiments (25 cooling cycles in five cats). For both parameters, changes were significant from the baseline level (Mann–Whitney *U* test; $P = 0.0006$ for response strength; $P < 0.0001$ for vector strength). (f) Orientation preference (Upper) and direction maps (Lower) obtained with oriented gratings, before (Left), during (Center), and after (Right) cooling pMS cortex. Note the stability of the orientation maps during the feedback deactivation, whereas the direction preference map exhibits pronounced changes of up to 180° . (g) Histograms of angular differences between direction maps obtained before and during (Left) and before and after (Right) pMS deactivation from the case shown in Fig. 2f. (Top) Angular differences for all pixel in the direction map. (Middle) Angular differences for the 30% pixel with the highest MDI (activity caused by the preferred direction minus the activation caused by the counterdirection). (Bottom) Angular differences for the 30% pixel with the lowest MDI. Note that even the group of pixel with a strong direction response (Middle) changes its direction preference during the feedback deactivation while regaining the initial preference after rewarming.

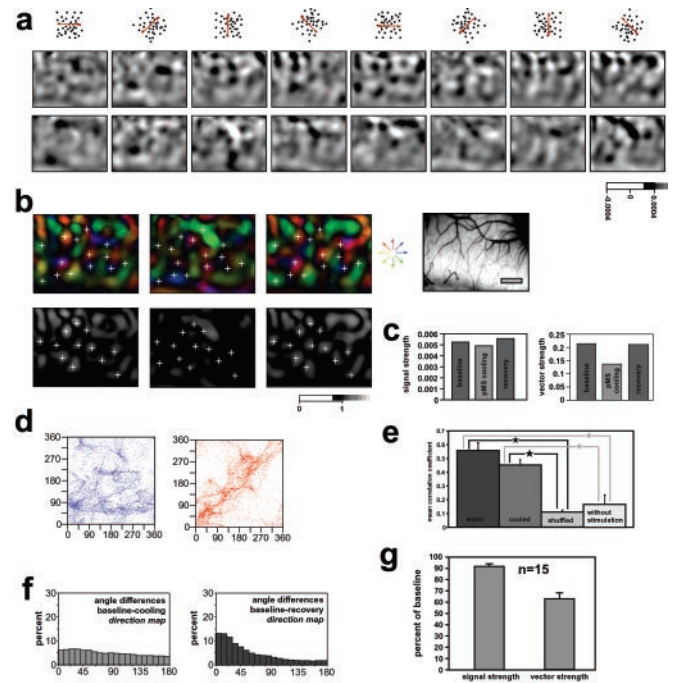


Fig. 3. Impact of feedback removal on direction maps: (a) Single-condition direction maps recorded in area 18 before (Upper) and during (Lower) cooling deactivation of the pMS cortex and stimulation with coherently moving random dots. The direction of movement for each set of images is indicated by the red arrow in the field of dots above each column. The gray scale below indicates the coding of the signal ranges. (b) Direction polar maps (Upper) and direction vector strength maps (Lower) before (Left), during (Center), and after (Right) cooling deactivation of pMS cortex from the experiment shown in a. Crosses indicate locations within the direction map that change direction preference and tuning strength during the cooling. (Right) Imaged region. (Bar = 1 mm.) (c) Averages of absolute signal and vector strengths during the three phases of a cooling cycle of the case illustrated in a and b. (d) Pixelwise comparison of the direction preferences between the direction maps shown in a and b. (Left) Direction preference before vs. cooling. (Right) Direction preference before vs. recovery. For many loci, there is very little correlation between direction preferences in the presence and absence of feedback signals ($r = 0.209$, $P < 0.0001$), whereas values are much more closely correlated for preferences calculated before and after feedback deactivation ($r = 0.582$, $P < 0.0001$). (e) Average correlation coefficients between direction preference maps recorded from individual frames within the sets of data recorded with intact feedback (dark gray) and during feedback deactivation (medium gray). The light-gray column indicates correlations between maps with and without feedback activity. The rightmost column indicates correlations between individual camera frames in control trials without visual stimulation. Note that there was only very low correlation between frames in the “warm” and “cooled” conditions (“shuffled”), whereas maps within each condition were stable over time. Note in addition that correlations among the frames without visual stimulation were markedly lower than among frames from trials with visual stimulation in the presence or absence of feedback activity. Differences in correlation between the “warm” and “cooled” condition were not significant (Mann–Whitney *U* test), whereas both conditions differed significantly from the “shuffled” and the “without stimulation” condition (Mann–Whitney *U* test, $P < 0.001$). (f) Angular differences between direction maps obtained before and during before and after pMS deactivation. Data are averaged across all experiments with random dots (15 cooling cycles in five cats). (Left) Histogram of the distribution of angular differences between direction maps recorded before and during cooling. Note that the histogram is nearly flat, indicating little systematic relation between the direction representations before and during cooling of pMS cortex. (Right) Histograms of the distribution of angular differences between direction maps recorded before and after cooling. Note that the distribution of angular differences peaks close to zero, indicating a good reproducibility for direction representation after the reinstatement of pMS feedback. (g) Changes in percent of baseline response strength and vector strength averaged over all experiments with random dots (15 cooling cycles in five cats). For both parameters, changes were significantly different from baseline level (Mann–Whitney *U* test; $P = 0.0038$ for response strength; $P = 0.0039$ for vector strength).

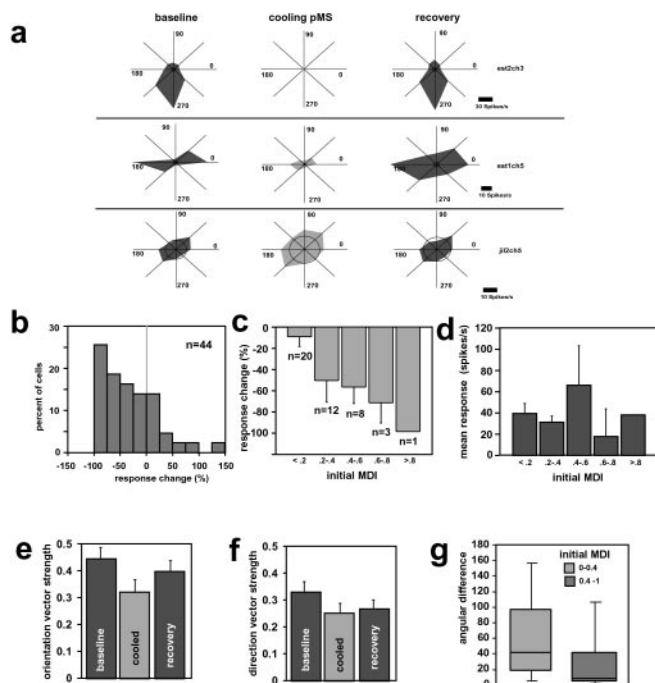


Fig. 4. (a) Polar plots of the spiking response of 3 units in area 18 before, during, and after deactivation of pMS cortex. The stimulus consisted of a set of eight unidirectionally drifting gratings. The inner ring in each polar plot indicates the level of spontaneous activity as measured over a period of 500 ms before stimulus onset. Note the complete silencing of a unit (*Top*), depressed activity of an orientation selective unit (*Middle*), and increased excitability of a relatively unselective unit (*Bottom*). (b) Histogram of the response changes induced by pMS cooling on the sample of 44 recorded units. Note that the large majority of units shows a response reduction during feedback inactivation. (c) Average response changes during pMS cooling separated according to their initial degree of direction selectivity. Impact of pMS cooling was greatest on neurons exhibiting higher degrees of direction selectivity (ref. 21; ANOVA, $P = 0.045$, $\alpha = 5\%$). (d) MDI was not related systematically to activity level. (e and f) Average changes of vector strength in the orientation and direction response of the recorded units. This parameter has been calculated in the same way as for the optical imaging results. For both parameters, changes were significant from the baseline level (Mann-Whitney U test; $P = 0.011$ for orientation; $P = 0.042$ for direction). (g) Box plots of angular changes in direction preference during feedback deactivation separated by their initial MDI. In these plots, the upper and lower borders of the filled part indicate the 75th and 25th percentiles, respectively; the lines above and below indicate the 90th and 10th percentiles, respectively; and the line within the body indicates the median of the distributions. Note that, in units with low MDI, direction changes in preferred direction and orientation were significantly more likely than in units with high MDI (Mann-Whitney U test; $P = 0.027$).

and that were then restored to full activity and direction selectivity on rewarming of the pMS cortex (Fig. 4a *Top*). Other neurons showed a reduction in response amplitude but without impact on orientation or direction selectivity (Fig. 4a *Middle*). Importantly, 30% of neurons in area 18 exhibited little or no change in activity during cooling of the pMS cortex, thus also verifying the absence of cooling effects on either the visual radiation or on area 18 directly (Fig. 4a *Bottom* and b). Sixty percent of area 18 upper-layer neurons exhibited a reduction in activity, and 10% showed an increase in activity during pMS cooling (Fig. 4b). Further analysis revealed that the impact of the deactivation was closely related to the initial degree of direction selectivity of the recorded neurons (Fig. 4c). The higher the initial degree of direction selectivity the stronger was the impact of feedback removal on the responsiveness of these neurons. In this context it is important to note that firing rates in our samples of neurons were not related to the degree of direction selectivity

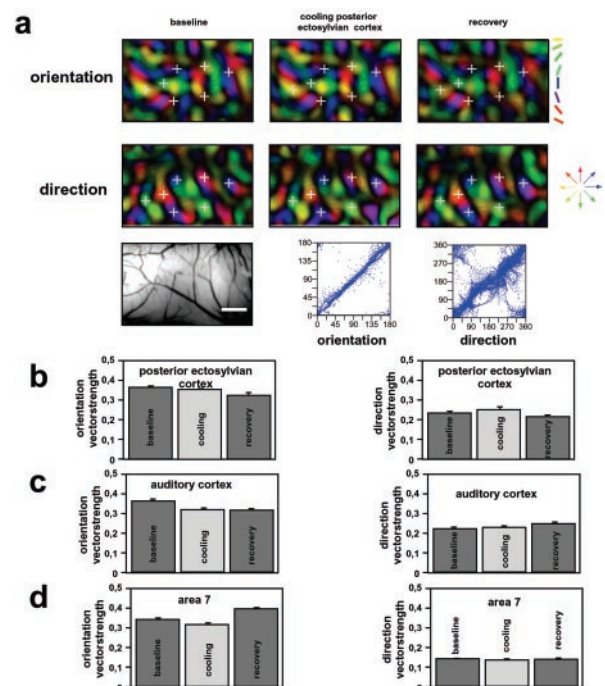


Fig. 5. Results from control coolings in cortical regions other than pMS. (a) Orientation (*Top*) and direction (*Middle*) polar maps from area 18 before, during, and after cooling deactivation of PE cortex (conventions as in Figs. 2 and 3). (*Bottom Left*) The imaged region. (Bar = 1 mm.) The plots beneath indicate the pixelwise comparison of orientation and direction preference between maps recorded before and during deactivation of PE cortex. Note the stability of these parameters during cooling. (b–d) Histograms of averaged orientation and direction vector strength before, during, and after inactivation of the PE cortex (b), auditory cortex (c), and area 7 (d). Note also here the stability of these parameters that were strongly affected by pMS deactivation during the cooling of the control sites.

of the respective cells (Fig. 4d). For neurons that remained visually responsive, orientation and direction selectivities, as measured by the vector strengths, broadened (Fig. 4e and f), and many changed their preferred direction (Fig. 4g). The most labile neurons were those with the initially lowest degree of direction selectivity. These electrophysiological data promote the view that changes in the direction map we identified with optical imaging are likely based on an actual change in preferred direction of less selective neurons in combination with the loss of highly directional responses.

Deactivation of Other Sites in the Cat Cerebral Cortex. Cooling deactivation of other cortices such as the posterior ectosylvian region of visuotemporal cortex (Fig. 5a), auditory cortex, or even area 7, which is interposed between MS sulcal cortex and primary visual cortex, had no or negligible impact on the imaged maps in area 18. Both the direction and the orientation representation in these areas remained unchanged and stable with respect to response strength and selectivity (Fig. 5 b–d). Thus, the impact of pMS cooling deactivation on the orientation and direction maps in area 18 does not result from a general depressive effect of cortical cooling on neural activity that is unrelated to cortical connectivity. Instead, they result from the silencing of a major transcortical pathway that feeds signals back from the pMS region of visuoparietal cortex to area 18, and the impact of these effects is greatest on the representation of visual motion.

Discussion

The electrophysiological and optical data are concordant, and both promote the view that changes in the direction map induced

by cooling deactivation of pMS cortex are based on: (i) actual changes in the preferred directions of less selective neurons and (ii) silencing, or near silencing, of neurons with the highest degree of direction selectivity. It is important to recognize that the functional impact of pMS deactivation on area 18 neurons reported in our study is high compared with prior studies on other cortical feedback systems (5–7, 23). The higher impact can be accounted for by the larger region of feedback pathway origin that was deactivated, a more effective deactivation that silences neurons in all layers in contact with the cooling loop, the high density of feedback projections from pMS cortex into upper layers of area 18, and emphasis of the electrophysiological and optical analyses on neurons in those same layers.

Methodological Considerations. Several lines of evidence assure us that the modifications we identified in the maps reflect changes in neuronal behavior in response to deactivation of a direct and specific feedback system. First, cooling deactivation of other cortices had little or no impact on the imaged maps in area 18. Additionally, previous studies have shown that the zone of direct cooling impact on cortex is confined to the banks of the MS sulcus (20), and direct thermal measurements in our experiments showed that temperatures fluctuated within area 18 by $<0.5^{\circ}\text{C}$ during cooling of pMS cortex. Second, there is negligible impact of the cooling on the optic radiations (18), a point verified by electrophysiological evaluation and vigorous responsiveness of visual fibers (24), and unaltered activity in a subpopulation of neurons in area 18 in our present recordings. Third, single-neuron recordings revealed changes in the response behavior that rule out map changes as a result of an uncoupling between neuronal and metabolic activity in area 18. That neuronal activity levels were reduced on average by only 10–15% during cooling ensures that the optical data obtained in the absence of pMS feedback are still based on considerable amounts of neuronal activity. Fourth, we can rule out that the changes in direction maps are based on alterations in the recording conditions that could have resulted in a poor signal-to-noise ratio. Direction maps recorded in the absence of feedback were stable over time, an observation we could not make when analyzing data obtained in the absence of cortical activation. Moreover, changes in direction maps have been observed with two different sets of stimuli, gratings and random dots, which cause different levels of cortical and direction specific activation (25) and, within individual maps, even at sites which exhibited a robust direction response. Finally, proficient behavioral performance on masked-pattern discrimination tasks, which depends on both primary visual and visuotemporal cortices, remains robust during cooling of MS cortex (24).

Feedback Impact on the Representation of Orientation. Our results show that feedback projections have a differential impact on two prominent visual representation systems in area 18. For the orientation system, feedback signals raise levels of neural activity and sharpen response selectivity but do not create orientation selectivity and its global representation in the form of maps. This conclusion fits previous data suggesting that orientation selectivity emerges largely by the convergence of specific sets of geniculocortical signals on layer IV neurons (1, 2, 26–30) and by local circuit amplification and sharpening of the selectivity (31–33). Because there is a paucity of feedback projections into layer IV, it is unlikely that pMS cortex has any significant impact on orientation construction at this level of visual processing. The first level where ascending and pMS feedback signals interact is in cortical layers II/III. Neurons in a radial translaminal column have similar orientation preferences (1, 34, 35), indicating that the map in layer IV is passed upward to neurons in layers II/III, where neurons have similar preferences to underlying neurons. However, response strength and selectivity do not appear to be transmitted faithfully from layer IV, and our electrophysiological and optical results show that upper-layer re-

sponses depend on feedback signals that selectively amplify ascending signals and sharpen orientation tuning, but without significant impact on orientation preference. Even though local circuits contribute to these processes (31, 34), several previous studies support our conclusions on the importance of feedback signal amplification in the form of gain enhancement for stimuli of low visibility (5), and for cortical feedback influences on neuronal activity in lateral geniculate nucleus (36–39). Moreover, such feedback amplification occurs contemporaneously with, or very soon after, initial neuron activation (6), supporting the idea that receptive fields are dynamic in both space and time (40–42).

Feedback Impact on the Representation of Movement Direction.

Besides the changes in response strength and selectivity, inactivation of pMS cortex induced profound changes in the overall representation of direction of motion in area 18. These alterations were probably based on the silencing of neurons with highly directional responses. By contrast to orientation, for direction selectivity there is no evidence that layer IV contains a refined map that approaches the order identified in the superficial layers (35, 43–45). Even though neurons in layer IV exhibit some direction selectivity (43), neurons above in the supragranular layers may have preferences that are diametrically opposite (35), and it seems likely that layer IV projections to layers II/III contribute little to the elaboration of direction selectivity in the latter layers (28, 46).

Prior studies designed to silence local circuits (32, 47, 48) have shown that local circuits modify direction preference in three ways: (i) by enhancing responses to movement in an existing preferred direction or activation of otherwise silent neurons; (ii) by increased excitation in a new direction; and (iii) by selective inhibition of largely unstructured activity. These same mechanisms may also apply to long-distance projections in generating direction selectivity, although evidence points to the first alternative as being dominant, because silencing of MS feedback projections severely reduces response magnitude, or even silences, the most direction-selective cells in area 18. The latter two possibilities are less well supported by our data, because we do not have strong electrophysiological evidence for changes in the preferred direction of highly direction selective neurons during deactivation of pMS cortex, and only few neurons exhibited a response enhancement during pMS deactivation.

Even though our results show that key features of the direction representation depend on substantial numbers of signals arriving from higher cortical areas, there is a caveat to our data. We used only a single temporal frequency and a single velocity for our tests on orientation and direction selectivity. In designing our stimuli, we needed to ensure that large numbers of both MS and area 18 neurons were activated well. However, the values selected (2 Hz and 16° per sec) may not be fully optimal for every MS and every area 18 neuron (11, 49, 50). We acknowledge that if we had used a fully comprehensive set of stimuli, we may have shown that the direction selectivities of every neuron in the upper layers of primary visual cortex was influenced by signals fed back from higher-motion cortices. However, we have shown that the majority of upper-layer neurons in area 18 depend on feedback projections from visuoparietal motion cortex for the emergence and full shaping of direction selectivity, and that these signals contribute in a major way to the full elaboration of direction maps.

We thank Sandra Schwegmann for outstanding technical assistance during the experiments; Thomas Maurer and Wilfried Zerb for skillful preparation of mechanical devices; Dr. Wolf Singer for encouraging and helpful support throughout the whole study; and Drs. Ulf Eysel and Zoltan Kisvárdy for discussions on the calculation of direction maps. This work was supported by the Max Planck Gesellschaft, the Deutscher Akademischer Austauschdienst, the National Science Foundation, and the National Institute of Neurological Disorders and Stroke.

1. Hubel, D. H. & Wiesel, T. N. (1962) *J. Physiol. (London)* **160**, 106–154.
2. Ferster, D. & Jagadeesh, B. (1991) *J. Neurophysiol.* **66**, 1667–1679.
3. Humphrey, A. L. & Saul, A. B. (1998) *J. Neurophysiol.* **80**, 2991–3004.
4. Martin, K. A. (1988) *Trends Neurosci.* **11**, 192–194.
5. Hupé, J. M., James, A. C., Payne, B. R., Lomber, S. G., Girard, P. & Bullier, J. (1998) *Nature* **394**, 784–787.
6. Hupé, J. M., James, A. C., Girard, P., Lomber, S. G., Payne, B. R. & Bullier, J. (2001) *J. Neurophysiol.* **85**, 135–145.
7. Wang, C., Walezczyk, W. J., Burke, W. & Dreher, B. (2000) *Cereb. Cortex* **10**, 1217–1232.
8. Salin, P. A. & Bullier, J. (1995) *Physiol. Rev.* **75**, 107–154.
9. Rudolph, K. K. & Pasternak, T. (1996) *Cereb. Cortex* **6**, 814–822.
10. Lomber, S. G., Payne, B. R., Cornwell, P. & Long, K. D. (1996) *Cereb. Cortex* **6**, 673–695.
11. Gizzi, M. S., Katz, E. & Movshon, J. A. (1990) *Visual Neurosci.* **5**, 463–468.
12. Zumbroich, T. J. & Blakemore, C. (1987) *J. Neurosci.* **7**, 482–500.
13. von Grünau, M., Zumbroich, T. J. & Poulin, C. (1987) *Vision Res.* **27**, 343–356.
14. Danilov, Y., Moore, R. J., King, V. R. & Spear, P. D. (1995) *Visual Neurosci.* **12**, 141–151.
15. Symonds, L. L. & Rosenquist, A. C. (1984) *J. Comp. Neurol.* **229**, 1–38.
16. Einstein, G. & Fitzpatrick, D. (1991) *J. Comp. Neurol.* **303**, 132–149.
17. Shipp, S. & Grant, S. (1991) *Visual Neurosci.* **6**, 339–355.
18. Lomber, S. G., Payne, B. R. & Horel, J. A. (1999) *J. Neurosci. Methods* **86**, 179–194.
19. Payne, B. R., Lomber, S. G., Geeraerts, S., van der Gucht, E. & Vandenbussche, E. (1996) *Proc. Natl. Acad. Sci. USA* **93**, 290–294.
20. Lomber, S. G. & Payne, B. R. (2000) *Cereb. Cortex* **10**, 1066–1077.
21. Orban, G. A., Kennedy, H. & Maes, H. (1981) *J. Neurophysiol.* **45**, 1043–1058.
22. Schuett, S., Bonhoeffer, T. & Hübener, M. (2001) *Neuron* **32**, 325–337.
23. Sandell, J. H. & Schiller, P. H. (1982) *J. Neurophysiol.* **48**, 38–48.
24. Lomber, S. G., Cornwell, P., Sun, J. S., MacNeil, M. A. & Payne, B. R. (1994) *Proc. Natl. Acad. Sci. USA* **91**, 2999–3003.
25. Galuske, R. A. W., Schmidt, K. E., Kluge, T. & Singer, W. (2001) *Soc. Neurosci. Abstr.* **31**, 164.2.
26. Reid, R. C. & Alonso, J. M. (1995) *Nature* **378**, 281–284.
27. Reid, R. C. & Alonso, J. M. (1996) *Curr. Opin. Neurobiol.* **4**, 475–480.
28. Malpeli, J. G. (1983) *J. Neurophysiol.* **49**, 595–610.
29. Malpeli, J. G., Lee, C., Schwark, H. D. & Weyand, T. G. (1986) *J. Neurophysiol.* **56**, 1062–1073.
30. Mignard, M. & Malpeli, J. G. (1991) *Science* **251**, 1249–1251.
31. Eysel, U. T., Muche, T. & Worgotter, F. (1988) *J. Physiol.* **399**, 657–675.
32. Somers, D. C., Todorov, E. V., Siapas, A. G., Toth, L. J., Kim, D. S. & Sur, M. (1998) *Cereb. Cortex* **8**, 204–217.
33. Crook, J. M., Kisvarday, Z. F. & Eysel, U. T. (1997) *Visual Neurosci.* **14**, 141–158.
34. Murphy, P. C. & Sillito, A. M. (1986) *J. Physiol.* **381**, 95–110.
35. Berman, N. E., Wilkes, M. E. & Payne, B. R. (1987) *J. Neurophysiol.* **58**, 676–699.
36. Schmielau, F. & Singer, W. (1977) *Brain Res.* **120**, 354–361.
37. McClurkin, J. W. & Marrocco, R. T. (1984) *J. Physiol.* **348**, 135–152.
38. Sillito, A. M., Jones, H. E., Gerstein, G. L. & West, D. C. (1994) *Nature* **369**, 479–482.
39. Przybyszewski, A. W., Gaska, J. P., Foote, W. & Pollen, D. A. (2000) *Visual Neurosci.* **17**, 485–494.
40. McLean, J. & Palmer, L. A. (1994) *Visual Neurosci.* **11**, 295–306.
41. DeAngelis, G. C., Ohzawa, I. & Freeman, R. D. (1995) *Trends Neurosci.* **18**, 451–458.
42. Ringach, D. L., Hawken, M. J. & Shapley, R. (1997) *Nature* **387**, 281–284.
43. Payne, B. R., Berman, N. E. & Murphy, E. H. (1981) *Brain Res.* **211**, 445–450.
44. Weliky, M., Bosking, W. H. & Fitzpatrick, D. (1996) *Nature* **379**, 725–728.
45. Shmuel, A. & Grinvald, A. (1996) *J. Neurosci.* **16**, 6945–6964.
46. Lee, C., Weyand, T. G. & Malpeli, J. G. (1998) *Visual Neurosci.* **15**, 27–35.
47. Pernberg, J., Jirrmann, K. U. & Eysel, U. T. (1998) *Eur. J. Neurosci.* **10**, 3596–3606.
48. Crook, J. M., Kisvarday, Z. F. & Eysel, U. T. (1996) *J. Neurophysiol.* **75**, 2071–2088.
49. Morrone, M. C., DiStefano, M. & Burr, D. C. (1986) *J. Neurophysiol.* **56**, 969–986.
50. Movshon, J. A., Thompson, I. D. & Tolhurst, D. J. (1978) *J. Physiol. (London)* **283**, 101–120.
51. Tusa, R. J., Rosenquist, A. C. & Palmer, L. A. (1981) in *Cortical Sensory Organization: Multiple Visual Areas*, ed. Woolsey, C. N. (Humana, Clifton, NJ), pp. 1–31.